**D2.5 Electrochemistry new findings**

| | | | | |
|---|---|---|---|---|
| **Reporting period** | from | **01.01.2022** | to | **31.03.2023** |
| **Report completed and released** | | **31.08.2022** | | |
| | | **Dominik Knapic, Achim Walter Hassel** | | |

## 1. Goals

The deliverable D2.5 is a public report published on the **LaserImplant** web-site (www.laserimplant.eu). on new findings about on electrochemistry of anodized and additionally ultrafast-laser processed Ti-based surfaces. It refers to a scientific article on these results.

## 2. Detailed Description

### 1. Introduction

Anodization processes were optimized for preanodization (before laser treatment) and for the anodization (after laser treatment) of the samples. For the preanodization a potentiostatic process was chosen, whereas for the anodization after the laser treatment a potentiodynamic process was studied. Ti6Al4V plates were treated by the femtosecond laser and anodized with different electrolytes. Additionally, 2 variations of samples were prepared, preanodized and subsequently femtosecond treated, and firstly femtosecond laser treated and subsequently anodized. Electrochemical and surface analysis were performed on the samples. Electrochemically active surface area (ECSA) was determined and oxide forming factors *k* were determined for 5 different electrolytes. Additionally, to determine the topography and morphology AFM (Atomic force microscopy), and Scanning electron microscopy (SEM) measurements were undertaken. Moreover, wettability was determined, and X-ray photoelectron spectroscopy (XPS) survey was conducted to investigate the electrolyte species incorporation in to the oxide produced by additional anodization. Finally, bioassessment with osteoblasts was undertaken.

### 2. Materials and Methods

#### 2.1. Sample preparation

#### 2.1.1. Samples anodized with different electrolytes

Ti6Al4V samples were ground with sandpapers with the grit sizes 220, 400, 600, 1000, 2500, 4000. Following the grinding, samples were polished with a silica paste (50 µm) resulting in a mirror like surface. Before femtosecond laser treatment, the samples were cleaned in ultrasonic bath in isopropanol and with distilled water, consequently.

The Ti6Al4V (Titanum grade 5) samples were structured with a femtosecond laser to produce micro cones and nanoripples on top of the cones. Specification of the laser: Spirit HE from Spectraphysics, 1040 nm wavelength, <350 fs pulse duration, Ytterbium based amplified fs-laser system, 100 mm focusing lens, focused beam diameter $2w_0$ = 75 µm. The following parameters were used for femtosecond laser treatment: peak fluence 2.77J $cm^{-2}$, (63 µJ pulse energy), 1 kHz repetition rate, 350 µm $s^{-1}$ scanning speed, line separation (meander pattern) = 20 µm.

Next, the samples were anodized potentiodynamically up to 10 V with a scan rate of 100 mV $s^{-1}$ in different electrolytes. The electrolytes used for anodization were: 0.1 M $H_2SO_4$, 25% $H_3PO_4$, 1 M phosphate buffer (pH=6.0), 1 M NaOH, 0.1 M citrate buffer (pH=5.79). One sample was not anodized and was used as a control sample.

Additionally, a sample was anodized up to 80 V with phosphoric acid as described before.

### 2.1.2. Preanodized samples

Pretreatment (grinding and polishing) for preanodization was the same as described above. The anodization process was carried out potentiostatically for 600 s, in a 25% phosphoric acid using a two-electrode setup. Ti6Al4V samples were anodized up to 100 V. The setup consisted of a TDK lambda Z+ power supply connected in series with a Keysight 34460A digital multimeter. The system was controlled via custom-made software which was developed in Labview. (Fig. 1).

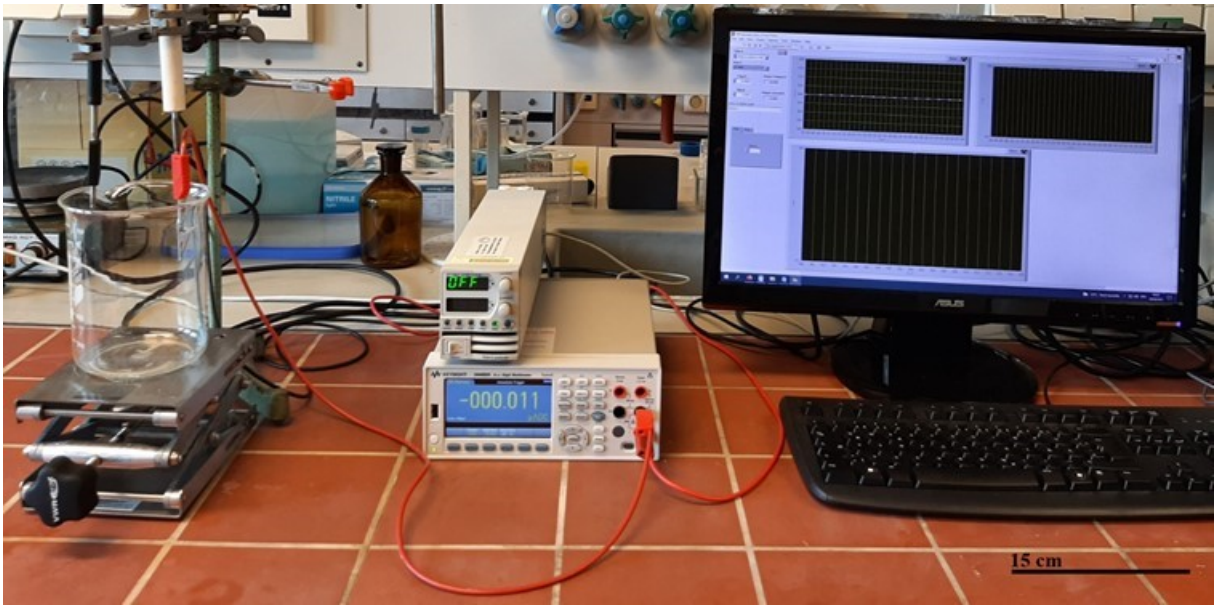


**Fig. 1:** Two electrode setup for potentiostatic anodization.

## 2.2. Electrochemical measurements

### 2.2.1. Electrochemically active surface area (ECSA)

To calculate the Electrochemically active surface area (ECSA), a comparison of total exchanged charge for anodization was done for polished Ti6Al4V femtosecond laser

structured, and preanodized samples. A series of cyclic voltammetry sweeps was conducted from $E_{vs\ SHE}$ = 0 V to $E_{vs\ SHE}$ = 5 V in steps of 0.5 V, total exchanged charge used for oxide growth was calculated from the CV curves.

### 2.2.2. Oxide forming factor *k*

An oxide forming factor was determined by calculating the thickness of the grown oxide by the total exchanged charge. For that a series of cyclic voltammetry sweeps was ran from $E_{vs\ SHE}$ = 0 V to $E_{vs\ SHE}$ = 5 V in steps of 0.25 V. To compare electrochemically obtained calculated values, a cross section on separately prepared samples was done with a FIB cut, and the thickness of the oxide was measured to calculate the oxide forming factor. Ti6Al4V samples were first ground and polished like described in 2.1.1. Followingly the samples were anodized in 25% $H_3PO_4$, 0.1 M $H_2SO_4$, 1 M NaOH, 0.1 M Citrate buffer (pH=5.79) and 1 M phosphate buffer (pH=6). The anodization was done potentiostatically for 600 s up to 50 V except for 1M NaOH that was anodized up to 40 V due to an excessive oxygen evolution.

## 2.3. Surface Characterization

The morphology of the structures obtained by the femtosecond laser treatment was determined by the EM Zeiss 1540 XB-Cross, FeldemREM. The topography of the samples was studied by the Nanosurf CoreAFM Atomic force microscope (AFM). The measurements were done in tapping mode. Following parameters were used: dynamic force, tip -Tap190Al-G, Image Size= 96.8 x 96.8 µm, Time / Line = 4 s, Points / Line = 1024, Free Vibration Amplitude = 3 V. The wettability was determined by the sessile droplet method using a 0.75 µL deionized water droplet. The images of the droplets were analyzed by the circle method in Matlab. Electrolyte species incorporation into the oxide was studied by the Thetaprobe Thermo Fisher X-ray photoelectron spectroscopy (XPS).

## 2.4. Bioassasment with osteoblasts

For the cell tests, bone-forming cells (osteoblasts) of the commercially available human cell line SAOS-2 (provider DSMZ—Deutsche Sammlung von Mikroorganismen und Zellkulturen GmbH, Braunschweig, Germany) were used. The cells were cultivated in an established cell culture medium in an incubator with a water vapor saturated atmosphere with 5% $CO_2$ content at 37 °C and were divided at a ratio of 1:10, once a week. After disinfection with ethanol, a set of samples were placed in a Petri dish with cells and culture medium, thus the samples were completely covered with liquid. After 8 days in the incubator, the cells at the samples were fixed and dehydrated. In detail, the cells were initially fixed overnight with 6% glutardialdehyde (GA; Merck, Darmstadt, Germany) in phosphate-buffered saline (PBS) and sub-sequently dehydrated with the help of ascending ethanol series (30%, 40%, 50%, 70%, 80%, 90%, 96%, 3 times 100%) for 30 min each. The samples were repeatedly transferred 3 times into 100% hexamethyl-disilazane (HMDS; Merck). After the overnight evaporation of HMDS, the samples were sputter-coated with gold and the cell density was evaluated by means of scanning electron microscopy (SEM).

## 3. Results and discussion

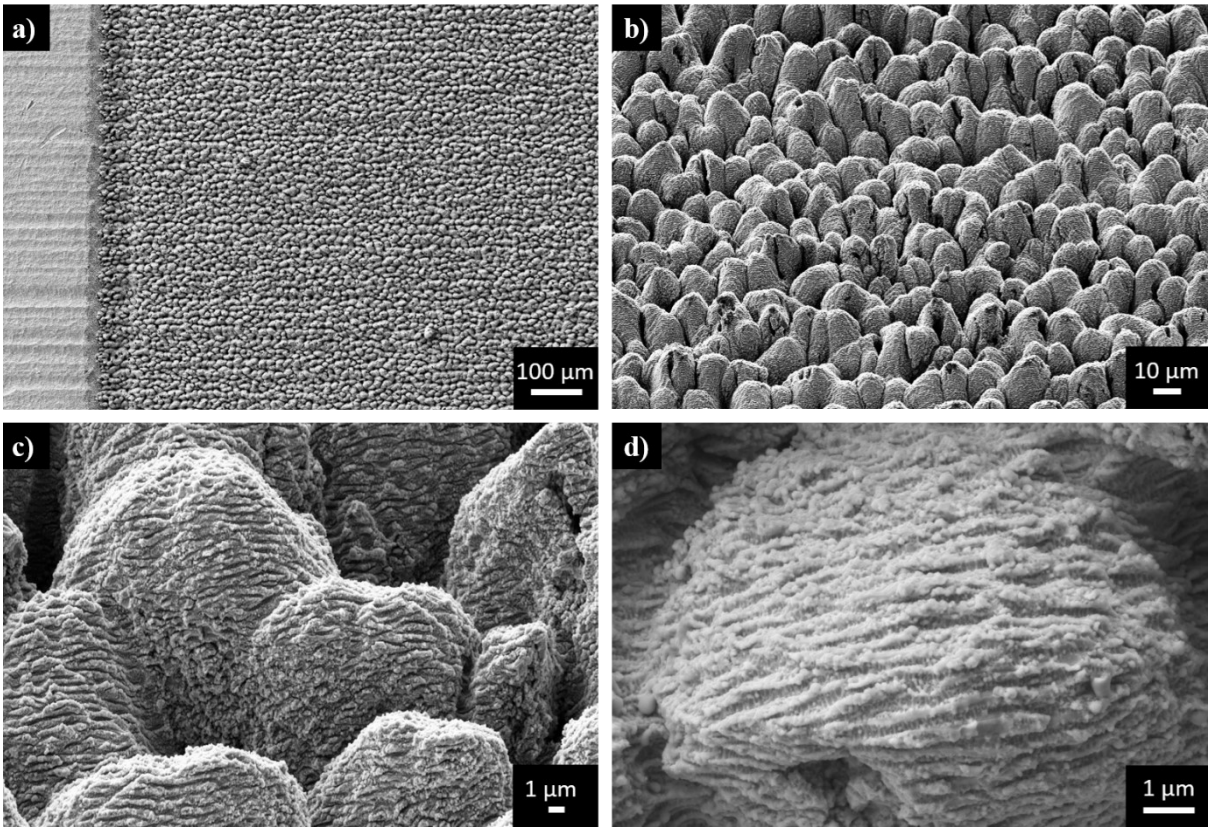


**Fig. 2:** Scanning electron microscopy (SEM) images of the femtosecond laser treated surface with micro-cones and nano-ripples.

Morphology was studied by the scanning electron microscopy. Fig. 2 shows the SEM images of the femtosecond laser treated surface at a tilt angle of 0° (a,b) and 45°(c,d). Treatment by an Ytterbium femtosecond laser at a < 350 fs pulse duration produced quasi -periodic micro cones structures and nano ripples on top of the cones. The cones structures are aligned with the direction of the scanning of the laser, forming rows which can be seen on Fig 2 a). Nano ripples that are grown on top of the micro cones are approximately 250 nm wide and parallel to each other forming a hierarchical surface morphology.

Furthermore, morphology of the preanodized femtosecond laser treated and anodized surfaces was investigated and compared. Comparing not preanodized and not anodized (0V_0V) (Fig 3 a)) and preanodized up to 100 V and not anodized (100V_0V) surface (Fig 3 b)), not anodized (100V_0V) surface showed bigger, and more compact ripples (grains) (Fig. 3). In Fig. 4 it can be seen that not preanodized and anodized with 10 V (0V_10V) surface has brighter surface, bigger ripples (grains) and more of the grains on top of the ripples have an additional oxide layer that can be clearly seen. Furthermore, Fig. 5 shows a surface of a not preanodized and anodized sample up to 80 V (0V_80V) that is overgrown with a more porous oxide layer and the ripples that are not distinguishable anymore.

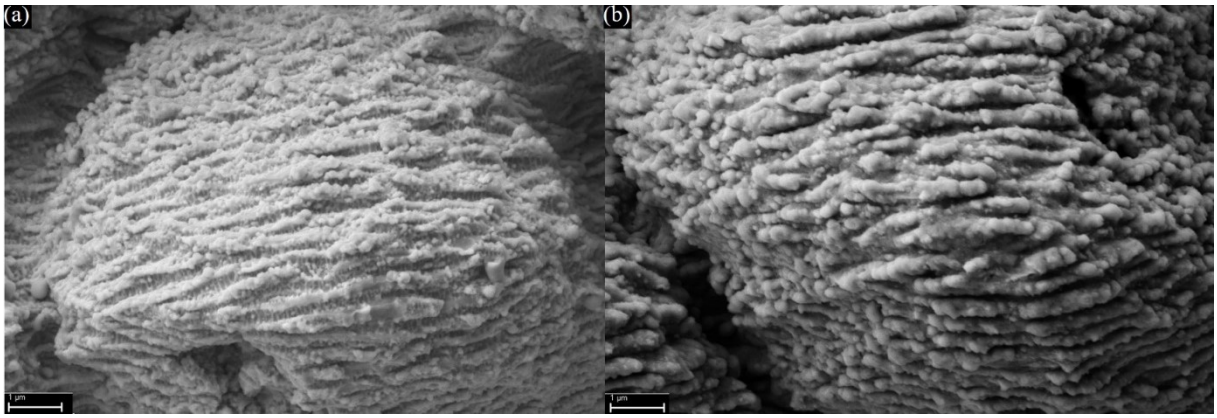


**Fig. 3:** a) SEM image of Ti6Al4V femtosecond laser treated sample not preanodized and not anodized (0V_0V); b) Preanodized up to 100 V and not anodized (100V_0V).

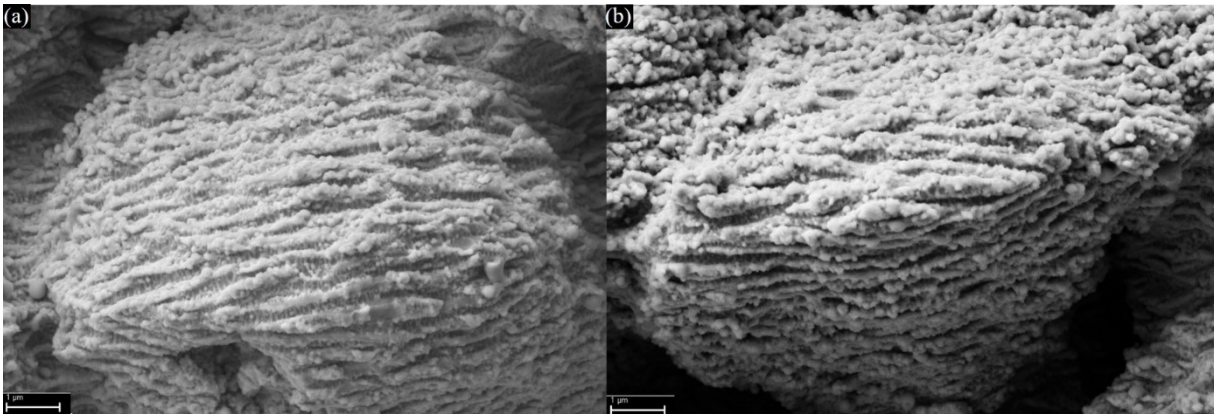


**Fig. 4:** a) SEM image of Ti6Al4V femtosecond laser treated sample not preanodized and not anodized (0V_0V); b) Not preanodized and anodized up to 10 V (0V_10V).

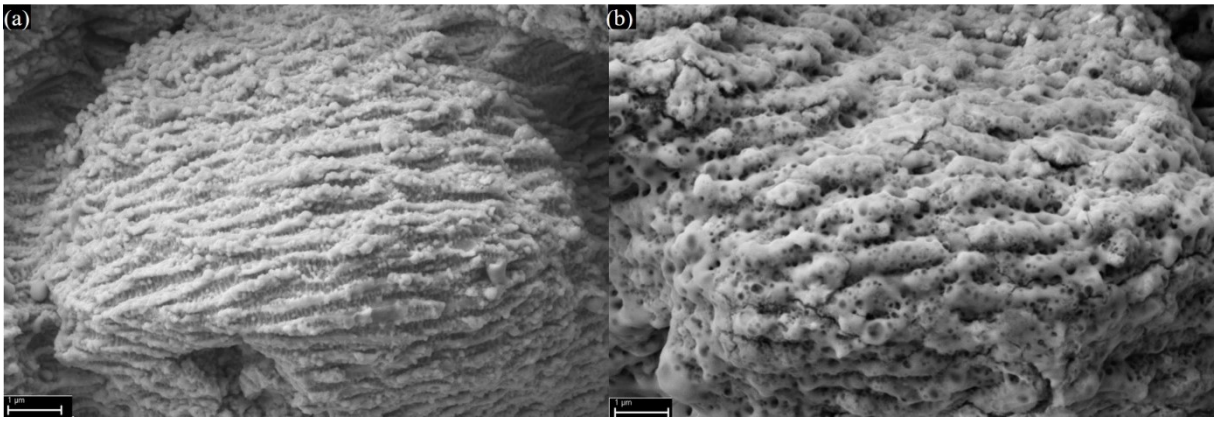


**Fig. 5:** a) SEM image of Ti6Al4V femtosecond laser treated sample not preanodized and not anodized (0V_0V); b) Not preanodized and anodized up to 80 V (0V_80V).

**Table 1.** Atomic force microscopy (AFM) parameters of laser treated surfaces combined with anodization in different electrolytes.

| | 0.1 M citrate buffer | 0.1M $H_2SO_4$ | 25% $H_3PO_4$ | 1M NaOH | 1 M phosphate buffer | not anodized |
|---|---|---|---|---|---|---|
| Average value / µm | 1.95 | 4.73 | 5.72 | 4.31 | 3.24 | 2.62 |
| Mean roughness (Sa) / µm | 1.35 | 1.50 | 1.55 | 1.60 | 1.48 | 1.07 |
| RMS roughness (Sq) / µm | 1.64 | 1.86 | 1.94 | 1.95 | 1.80 | 1.32 |
| Maximum height (Sz) / µm | 8.23 | 9.63 | 11.55 | 9.87 | 8.95 | 6.85 |
| Projected area / µm² | 9370 | 9370 | 9370 | 9370 | 9370 | 9370 |
| Surface area / µm² | 12892 | 13275 | 14705 | 12524 | 13605 | 12017 |
| Volume / µm³ | 18287 | 44323 | 53594 | 40353 | 30348 | 24555 |

Moreover, the topography was studied by means of Atomic force microscopy. 3D images of the samples can be seen on the Fig. 6., from the scans it can be concluded that each sample has a different topography. Consequently, different roughness's were determined for each sample, ranging from 1.32 µm for the not anodized sample to 1.95 µm for the sample anodized with 1M NaOH. Measured surface area ranged from 12017 µm$^2$ for the not anodized sample and 14705 µm$^2$ for 25% $H_3PO_4$, which is 28 % and 57 % more than the projected area. (Table 1)

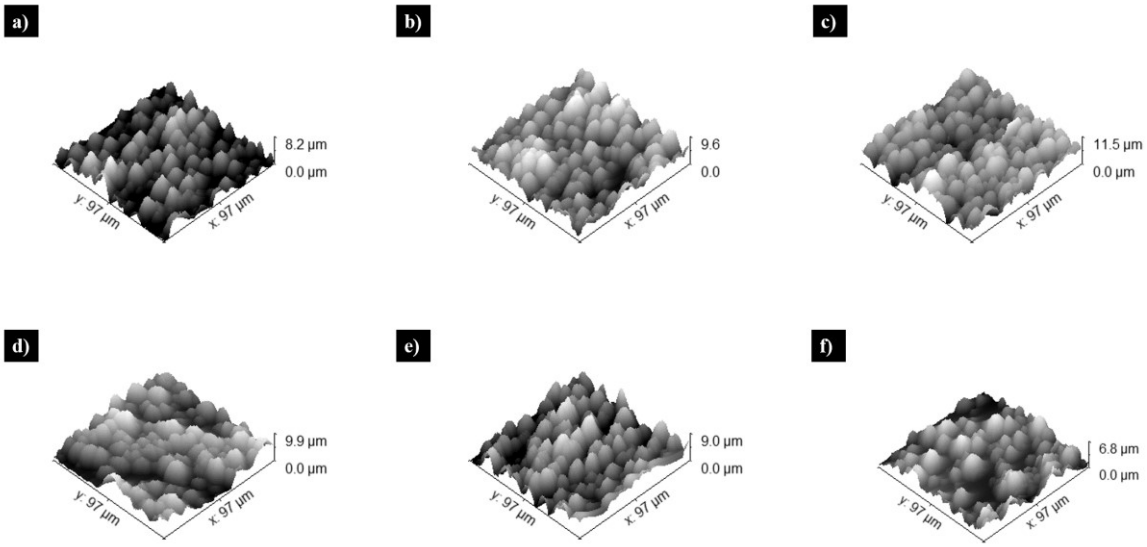


**Fig. 6:** Atomic force microscopy 3D images of laser treated surfaces; f) without anodization and surfaces anodized with: a) 0.1 M citrate buffer, b) 0.1 M $H_2SO_4$, c) 0.25 $H_3PO_4$, d) 1 M NaOH, e) 1 M phosphate buffer.

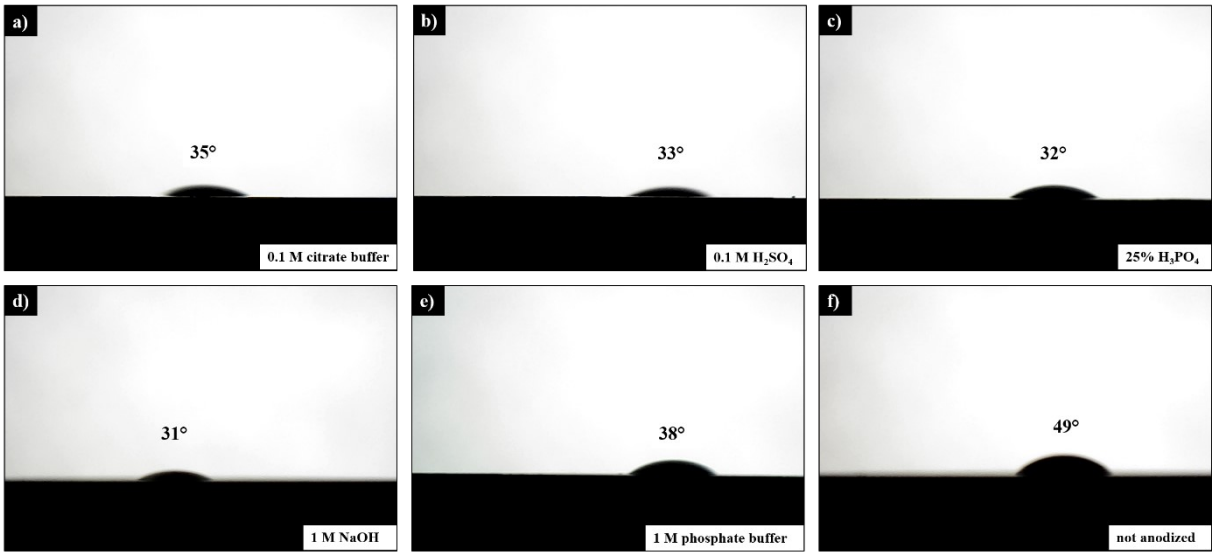


**Fig. 7:** Images of droplet formed on a laser treated surface combined with anodization in different electrolytes.

Furthermore, wettability was studied by the droplet contact angle experiment. From the results (Fig. 7) it is seen that the not anodized sample has the highest contact and is therefore the least wettable, whereas the most wettable is the sample anodized with 1 M NaOH. The contact angle was plotted against the root mean square roughness (RMS) (Fig. 8). A clear trend of reverse proportionality of contact angle to RMS can be observed. Which consequently is a proportionality of the wettability to RMS.

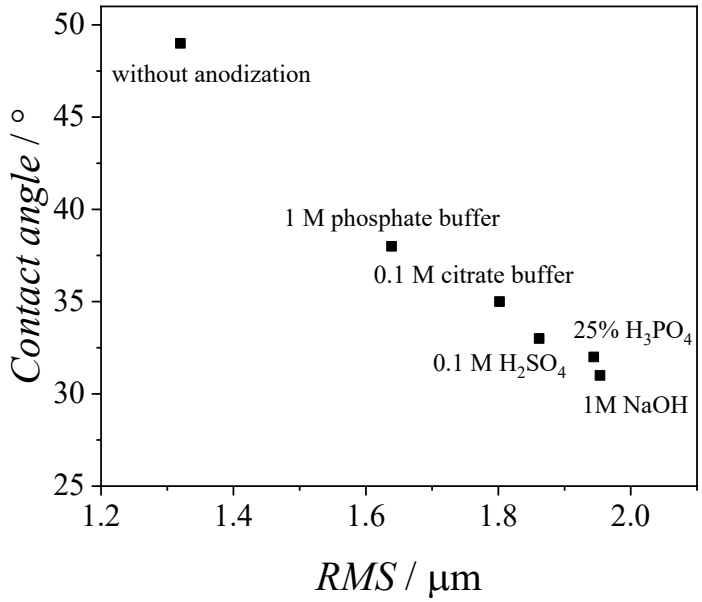


**Fig. 8:** Contact angle vs. root mean square roughness (RMS) formed on a laser treated surface combined with anodization in different electrolytes.

Electrochemically active surface area (ECSA) was determined by comparing a total exchanged charge used in a series of cyclic voltammetry series (Fig. 9**).** By comparing the total exchanged charge used to anodize mirror like polished bulk Ti6Al4V with a preanodized and laser treated and only laser treated sample, it can be seen that the used charge for a preanodized sample is 10 times larger, and for the only laser treated 14 times larger than for a polished bulk. This indicates that the oxide produced by the laser treatment on a preanodized sample has less defects that can be “fixed” by the additional anodization. On contrary, a sample with only laser treatment used more charge for anodization, therefore this indicates that the oxide has more defects. This can be explained by the fact that for the preanodized sample the oxide grown by the laser grows from the surface with already existing oxide layer with an approximated thickness of 150 nm. When the ECSA is compared to the measured surface by the AFM (Table 1) a considerable difference can be observed. One possible explanation could be that due to the high porosity of the oxide layer an AFM can simply not detect all of the area that could be under the surface. Additionally, the AFM imaging was limited with the resolution of 95 µm, and could not detect fine nanostructures which can significantly influence the surface area.

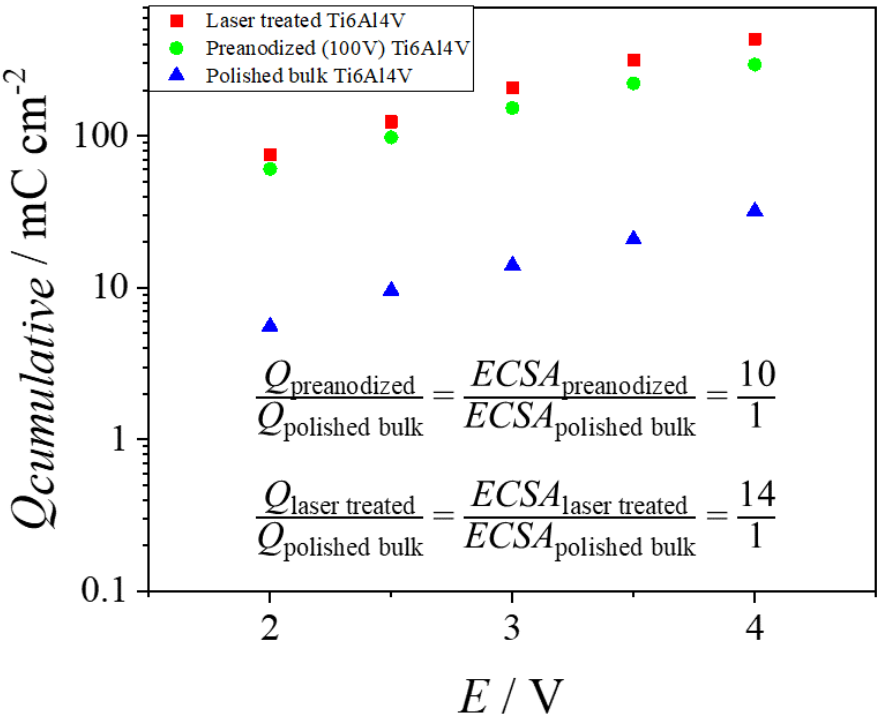


**Fig 9:** Cumulative charge used for oxide growth vs. potential for the preanodized, only laser treated Ti6Al4V, and polished Ti6Al4V.

To further investigate the oxide layer properties, the oxide forming factors for different electrolytes were determined electrochemically and later compared with values obtained by measuring the thickness from the cross section. In order to calculate the oxide forming factor *k*, a series of CV´s in the range of 0 V to 5 V and in steps of 0.5 V were done (Fig. 10). If the electrical current *I* is plotted against the time t, total exchanged charge Q can be determined using the following equation; $Q = \int \boldsymbol{I\,dt}$. Furthermore, from the equation $d=\frac{\boldsymbol{Q\,V_M}}{\boldsymbol{A\,z\,F}}$, an oxide thickness *d* can be calculated. When the oxide layer thickness *d* is plotted against potential *E*, from the slope of the plot *d* = *k E*, an oxide forming factor *k* can be determined (Fig. 11).

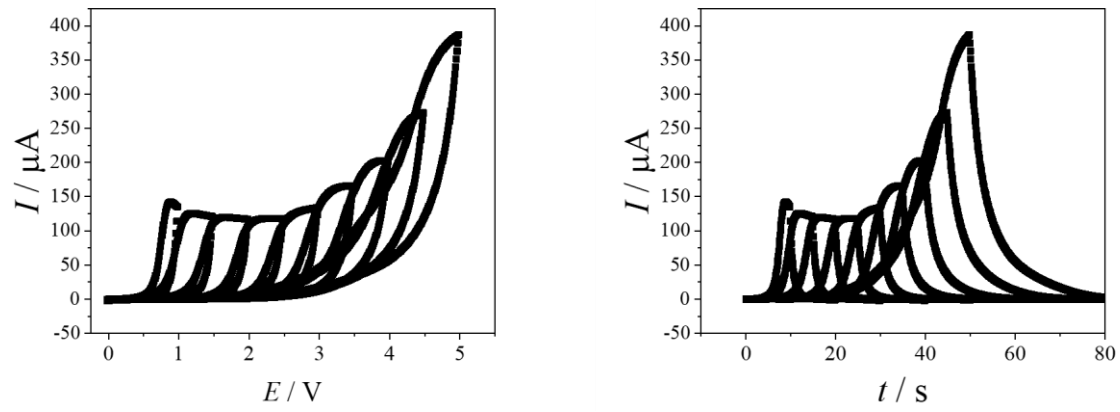


**Fig. 10:** Cyclic voltamograms (CV´s) of polished Ti6Al4V (Titanum grade 5) sample.

The oxide forming factors calculated electrochemically, were compared by the oxide forming factors obtained from the oxide thickness measured from the cross section. The lowest value of the *k* factor was obtained for the 1M phosphate buffer and it was 1.3 V $s^{-1}$ and 1.4 V $s^{-1}$ obtained electrochemically and by measuring the cross section. The highest value was obtained for the 1M NaOH and it was 2.0 V $s^{-1}$ for both values. The different values of the *k* factors show that the oxide grown by the different electrolytes has different thicknesses which can also have some influence on the osteoblast growth.

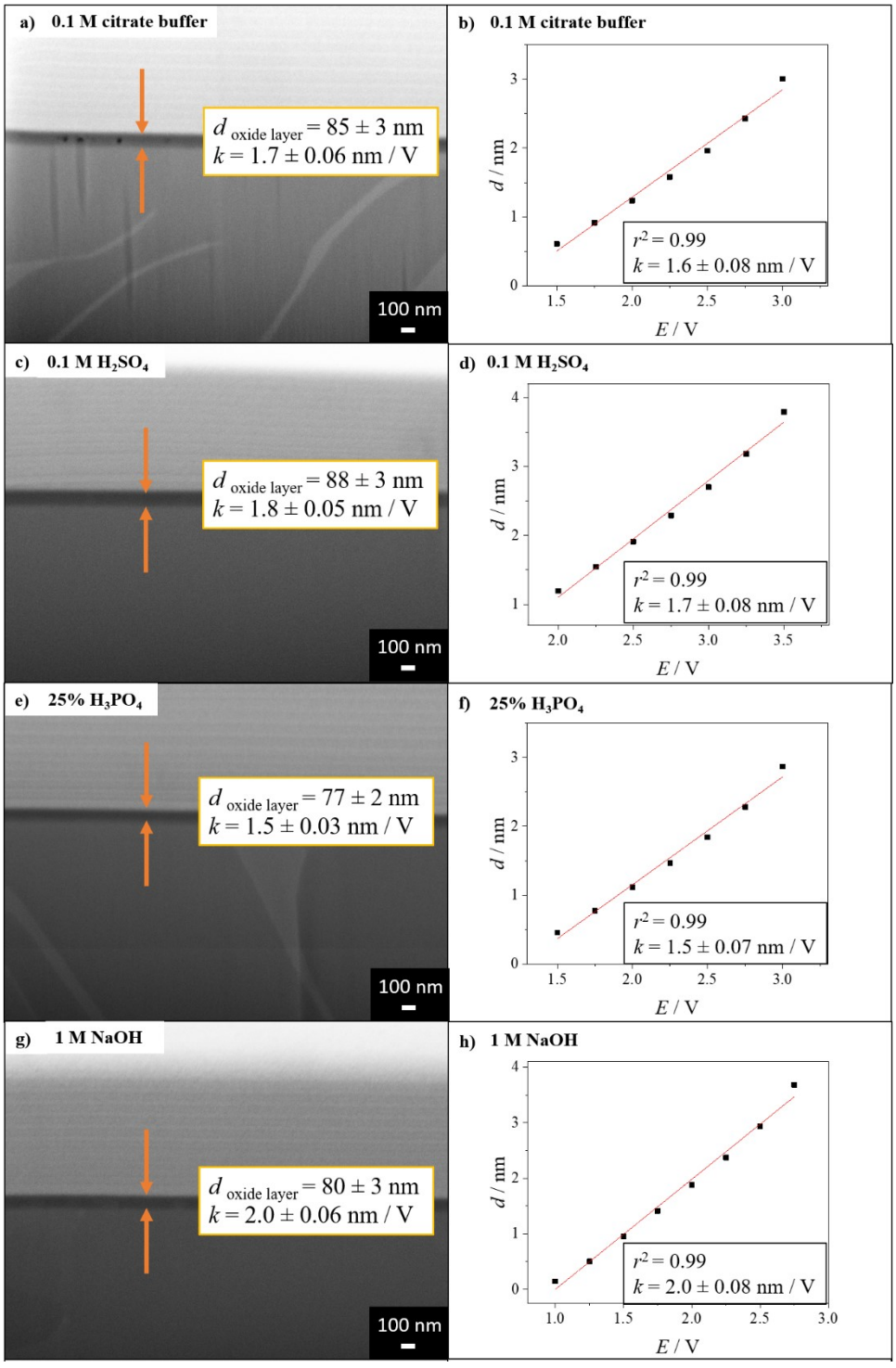

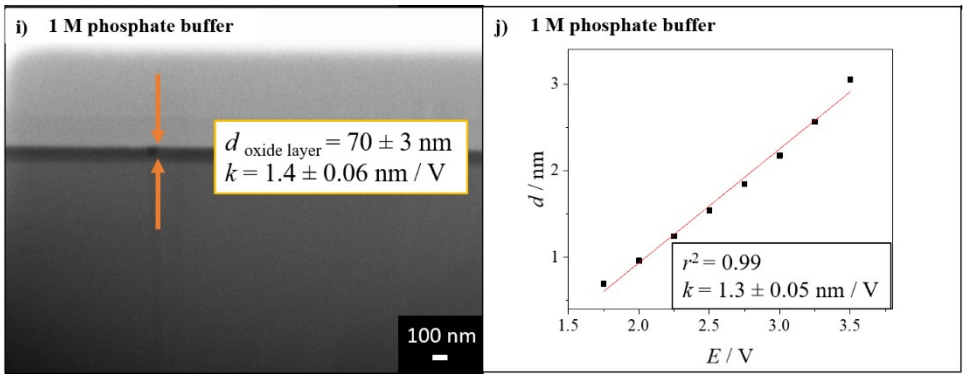


**Fig. 11:** Oxide forming factors *k* obtained from the measuring the thickness by the cross section and electrochemically obtained oxide forming factors for different electrolytes.

Next, bioassessment with osteoblast was undertaken on laser treated Ti6Al4V samples anodized with different electrolytes and on one spot that was not anodized as a control sample. Surface anodized with 0.1 M citrate buffer (Fig. 12 a)) produced an osseorepellent surface whereas the surface anodized with 0.1 M $H_2SO_4$ (Fig. 12 c)) produced a surface that activates the growth of osteoblast. Surfaces anodized with 25% $H_3PO_4$ (Fig. 12 d)), 1 M phosphate buffer (Fig. 12 e)), 1 M NaOH (Fig. 12 f)) did not show significant difference in growth compared to the not anodized surface.

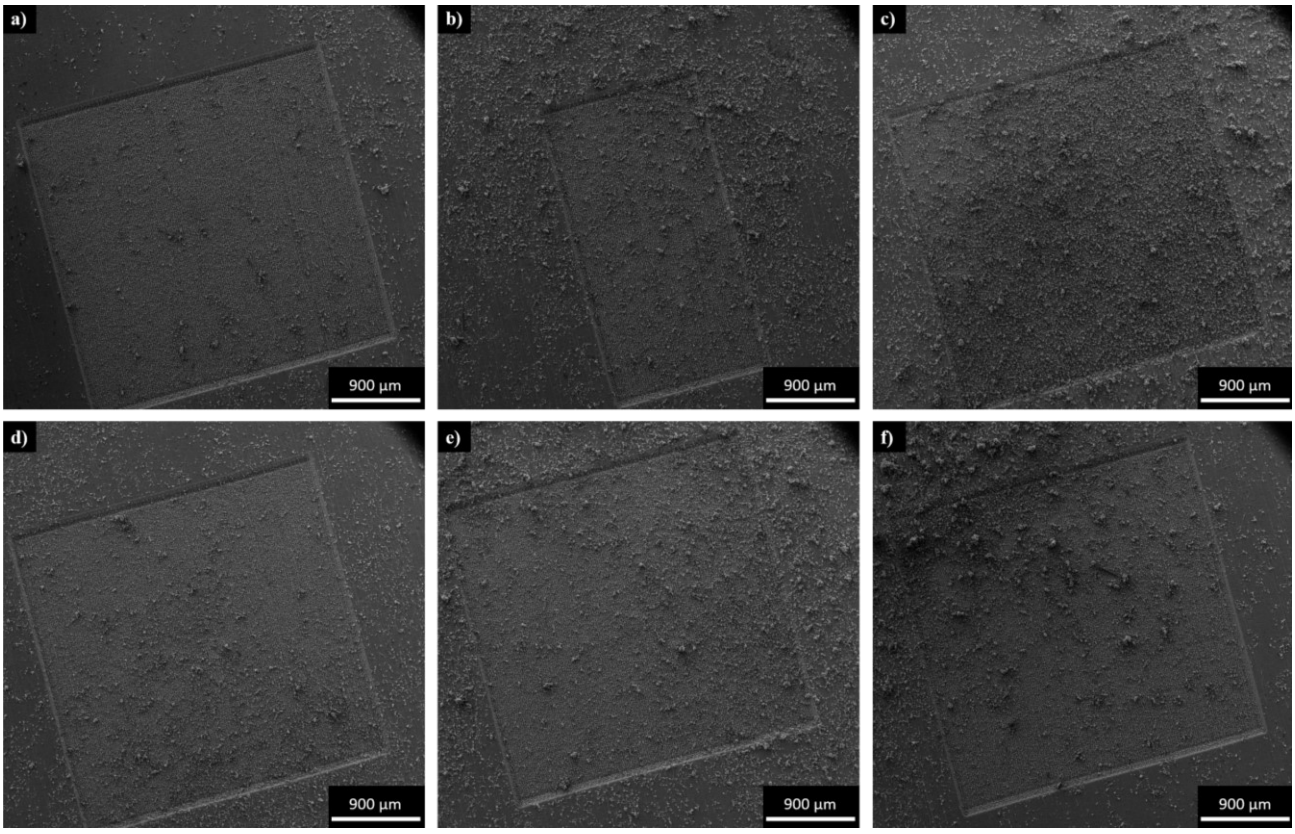


**Fig. 12:** Scanning electron microscopy (SEM) images of osteoblast cells grown on a laser treated surface; b) without anodization and surfaces anodized with: a) 0.1 M citrate buffer, c) 0.1 M $H_2SO_4$, d) 25% $H_3PO_4$, e) 1 M phosphate buffer, f) 1 M NaOH.

Finally, to study the incorporation of the electrolyte species into the oxide layer an XPS survey was conducted for the 0.1 M citrate buffer and 0.1 M $H_2SO_4$. It was found that in both cases

no electrolytes species were incorporated in the oxide layer formed anodically on top of the laser treated sample. (Fig. 13, Fig. 14)

In the end, it can be concluded that not a single parameter such as surface roughness, wettability, oxide thickness or the composition of the oxide could be singled out as the most influencing on the osteoblast growth, but a synergy of all of them influences the growth of the osteoblast.

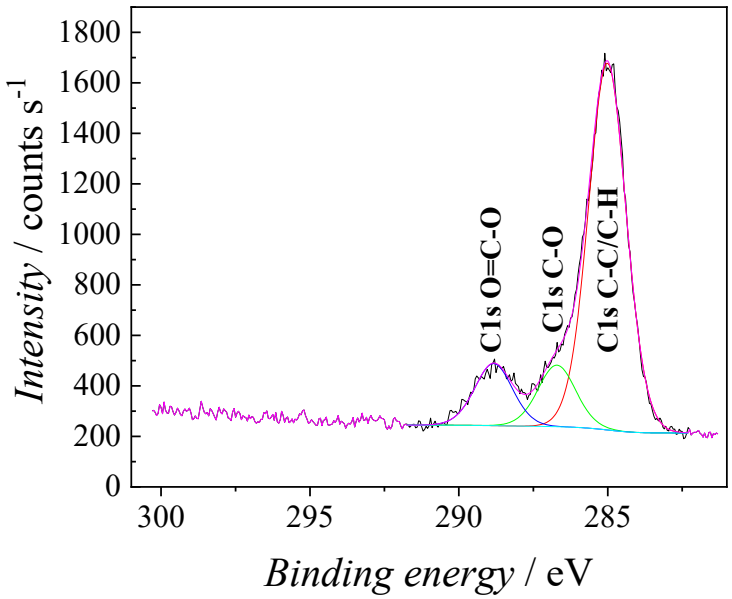


**Fig. 13:** X-ray photoelectron spectroscopy (XPS) spectra of laser treated surface anodized with 0.1 M citrate buffer.

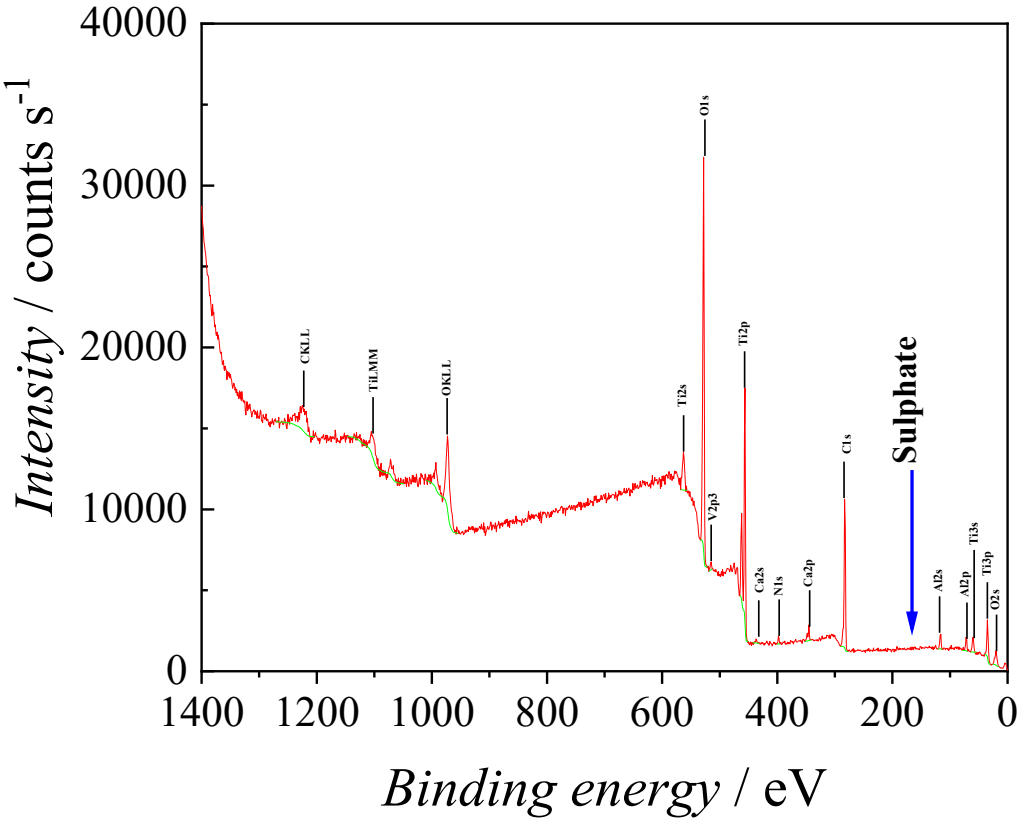


M

## 3. Evaluation of Goals and Resulting Actions

The deliverable **D2.5 Electrochemistry new findings** was finalized in time by m20. A link to this report will be implemented into the Dissemination section of the **LaserImplant** web-site (www.laserimplant.eu).

The results of this deliverable were presented as poster / contributed talk at the conference Engineering of Functional Interfaces ,Maastricht and are planned to be published in the frame of a scientific article in the journal physica status solidi a.

This report is part of the project **LaserImplant** that has received funding from the European Union's Horizon 2020 research and innovation programme under grant agreement No. 951730.